Journal of Radiation Research, Vol. 58, No. 3, 2017, pp. 363–371
doi: 10.1093/jrr/rrw088
Advance Access Publication: 25 October 2016

Lifetime attributable risk of radiation-induced secondary cancer from proton beam therapy compared with that of intensity-modulated X-ray therapy in randomly sampled pediatric cancer patients

Masaya Tamura[1], Hideyuki Sakurai[2], Masashi Mizumoto[2], Satoshi Kamizawa[2], Shigeyuki Murayama[3], Haruo Yamashita[3], Seishin Takao[4], Ryusuke Suzuki[4], Hiroki Shirato[1,5] and Yoichi M. Ito[6*]

[1]Department of Radiation Medicine, Hokkaido University Graduate School of Medicine, Kita 15, Nishi 7, Kita-ku, Sapporo, 060-8638, Japan
[2]Proton Medical Research Center, University of Tsukuba, Amakubo 2-1-1, Tsukuba, 305-8576, Japan
[3]Proton Therapy Division, Shizuoka Cancer Center Hospital, 1007 Shimonagakubo, Nagaizumi, Shizuoka, 411-8777, Japan
[4]Department of Medical Physics, Hokkaido University Hospital, Kita 14, Nishi 5, Kita-ku, Sapporo, 060-8648, Japan
[5]Quantum Medical Science and Engineering, Hokkaido University Graduate School of Medicine, Kita 15, Nishi 7, Kita-ku, Sapporo, 060-8638, Japan
[6]Department of Biostatistics, Hokkaido University Graduate School of Medicine, Kita 15, Nishi 7, Kita-ku, Sapporo, 060-8638, Japan
*Corresponding author. Department of Biostatistics, Hokkaido University Graduate School of Medicine, Kita 15, Nishi 7, Kita-ku, Sapporo, 060-8638, Japan. Tel: +81-11-706-5896; Fax: +81-11-706-6050; Email: ito-ym@med.hokudai.ac.jp
Received May 25, 2016; Revised August 1, 2016; Accepted August 5, 2016

ABSTRACT

To investigate the amount that radiation-induced secondary cancer would be reduced by using proton beam therapy (PBT) in place of intensity-modulated X-ray therapy (IMXT) in pediatric patients, we analyzed lifetime attributable risk (LAR) as an *in silico* surrogate marker of the secondary cancer after these treatments. From 242 pediatric patients with cancers who were treated with PBT, 26 patients were selected by random sampling after stratification into four categories: (i) brain, head and neck, (ii) thoracic, (iii) abdominal, and (iv) whole craniospinal (WCNS) irradiation. IMXT was replanned using the same computed tomography and region of interest. Using the dose–volume histograms (DVHs) of PBT and IMXT, the LARs of Schneider *et al.* were calculated for the same patient. All the published dose–response models were tested for the organs at risk. Calculation of the LARs of PBT and IMXT based on the DVHs was feasible for all patients. The means ± standard deviations of the cumulative LAR difference between PBT and IMXT for the four categories were (i) 1.02 ± 0.52% ($n = 7$, $P = 0.0021$), (ii) 23.3 ± 17.2% ($n = 8$, $P = 0.0065$), (iii) 16.6 ± 19.9% ($n = 8$, $P = 0.0497$) and (iv) 50.0 ± 21.1% ($n = 3$, $P = 0.0274$), respectively (one tailed *t*-test). The numbers needed to treat (NNT) were (i) 98.0, (ii) 4.3, (iii) 6.0 and (iv) 2.0 for WCNS, respectively. In pediatric patients who had undergone PBT, the LAR of PBT was significantly lower than the LAR of IMXT estimated by *in silico* modeling. Although a validation study is required, it is suggested that the LAR would be useful as an *in silico* surrogate marker of secondary cancer induced by different radiotherapy techniques.

KEYWORDS: radiation-induced, secondary cancer, proton beam therapy, intensity-modulated radiotherapy, lifetime attributable risk

INTRODUCTION

Intensity-modulated X-ray therapy (IMXT) can achieve excellent dose conformation, even to irregularly shaped target volumes, compared with 3D radiotherapy. Proton beam therapy (PBT) can achieve conformal irradiation similar to or better than IMXT. Since PBT can reduce the low dose regions outside the target volume compared with IMXT, it is generally thought that the risk of radiation-induced secondary cancer is lower for PBT than for IMXT [1]. However, it has been estimated that a period of at least 30 years would be needed to observe the difference in the incidence of radiation-induced secondary cancer between PBT and IMXT [2]. Since such a long follow-up period is not practical for a prospective clinical study, surrogate markers for the incidence of radiation-induced secondary cancer are strongly warranted.

To find a cost-effective way to select patients who should be treated by PBT rather than IMXT, a model-based approach using normal tissue complication probability calculations was recently reported for adult cancers [3]. It may also be reasonable to estimate the risk of secondary cancers when selecting pediatric patients for treatment using PBT rather than IMXT. A surrogate marker for secondary cancer based on scientific models and proper parameters is required for this purpose. Schneider *et al.* suggested that dose distribution data from a 3D radiation treatment planning system (3DTPS) based on computed tomography (CT) images could be used to estimate the lifetime attributable risk (LAR) of secondary cancer after radiation therapy [4]. The LAR is based on a long-term observation study of the atomic bomb survivors in Hiroshima and Nagasaki [5] and of patients who have received radiotherapy for Hodgkin's disease [6]. In this study, we investigated whether the LAR could be used as an *'in silico'* surrogate marker for any pediatric cancers, by examining the amount of difference in the LAR between the different dose distributions for PBT and IMXT in the same patient.

Applying the method of Schneider *et al.*, we examined the difference in LAR between PBT and IMXT, using the 3DTPS data for pediatric patients with tumors who had received PBT in two Japanese institutions. There have been several reports for whole craniospinal (WCNS) irradiation using the same method, where the difference would be largest. To date, there have been studies showing that the LAR obtained with PBT is lower than that obtained with IMXT using a representative scenario for optic glioma and vertebral body Ewing's sarcoma [7], or brain/head and neck tumors [8], or WCNS [1, 9–11]. However, it has not been certain whether the difference in LAR between PBT and IMXT is generally observed for pediatric patients in any treatment sites or just occurs in selected patients. To answer this question, in this study we randomly sampled patients from all pediatric patients who were treated using PBT in two representative institutions in Japan. In addition, by applying different dose–response models to individual patients, we evaluated how much the difference between PBT and IMXT would change according to the selected model.

MATERIALS AND METHODS

Calculation of LAR

There have been three dose–response models applied for determining the relationship between dose and the risk of radiation-induced secondary cancer: the linear model, the bell-shaped model and the plateau model (see Supplementary data). The various organs have been reported to be best fitted by one or another of these models [12–17]. Schneider *et al.* have proposed a 'full model', which integrates all three models into one equation [18]. By changing the parameters in the full model, we can estimate the effect of the different dose–response models on the LAR, which is based on dose–response models as follows:

$$RED(D) = \frac{e^{-\alpha' D}}{\alpha' R}\left(1 - 2R + R^2 e^{\alpha' D} - (1-R)^2 e^{-\frac{\alpha' R}{1-R}D}\right) \quad (1)$$

$$\alpha' = \alpha + \beta\frac{d_f}{D_T}D.$$

Here, D is the dose, R and α' are organ-specific model parameters (where R is the repopulation parameter and α' the cell kill parameter), D_T is the prescribed dose and d_f is the fraction dose.

For sarcoma induction, the following formula was used:

$$RED(D) = \frac{e^{-\alpha' D}}{\alpha' R}\left(1 - 2R + R^2 e^{\alpha' D} - (1-R)^2 e^{-\frac{\alpha' R}{1-R}D} - \alpha' RD\right). \quad (2)$$

Computed tomography (CT) and 3DTPS are used to calculate D, the dose at a certain point in the organ at risk (OAR). The dose–volume histogram (DVH) of the OAR derived using the CT data is patient-specific and treatment-specific. Therefore, the DVH can be used to calculate the total risk of secondary cancer of the OARs in the patient by the following equation.

As the total risk of secondary cancer in the OAR, the organ equivalent dose (OED) is calculated using DVH and *RED* as follows:

$$OED = \frac{1}{V_T}\sum_i V(D_i)RED(D_i), \quad (3)$$

where V_T is the total organ volume and $V(D_i)$ the dose–volume histogram.

Using the age at exposure to radiotherapy and the age attained, excess absolute risk (EAR) at the age attained can be obtained as follows (Eq. 4). Parameters in the equation were based on the previously published cancer risk data from A-bomb survivors [5, 19] and patients receiving radiation therapy for Hodgkin's disease [13, 15, 20]:

$$EAR(D, e, a, s) = OED \cdot \beta_{JP} \cdot \exp\left(\gamma_e(30 - e) + \gamma_a \ln\left(\frac{a}{70}\right)\right) \cdot (1 \pm s), \quad (4)$$

where β_{JP} is the initial slope of the A-bomb survivors, e the age at exposure, a the age attained, γ_e, γ_α the age modifying parameters, and s a gender-specific factor (0.17 and −0.17 for females and males).

To calculate the risk of secondary cancer throughout the patient's life, *LAR* can be calculated as follows (Eq. 5):

$$LAR(D, e, a) = \int_{a=e+L}^{a_{max}} EAR(D, e, a, s) \cdot \frac{s(a)}{s(e)} da. \quad (5)$$

Here, $(a)/(e)$ is the probability of surviving from age e to age a, and L is the latent period for solid cancer induction (5 years for solid cancer and 2 years for leukemia).

The parameters used in the calculation were derived from the study of Schneider *et al.* [4]. However, since there were no data about the thyroid in this paper, data from another paper by Schneider using a bell-shaped model were used [15]. In the previous paper, the β value in the EAR calculation was derived from the data transformed to be applicable for patients in UK [21]. However, since all the patients in this study were Japanese, we used the original data from Japanese atomic bomb survivors in this study. The integral area of LAR was from the attained age plus 5 to 75 years. In addition, the (a) and (e) values were taken from the 2011 Japanese life table rather than from the American data in the Schneider's paper.

In the case that more than one dose–response curve was available, we calculated the LAR for each dose–response curve along with the load average of the LAR as the LAR for this patient.

The parameters used in this study is listed in Table 1 for carcinoma and Table 2 for sarcoma.

Sampling of the patients

Subjects consisted of 242 patients who were <20 years old and for whom 3DTPS data were available; these 242 subjects included 143 patients who had been treated using PBT at Tsukuba University Hospital between 2009 and 2014 and 99 patients at the Shizuoka Cancer Center who had been treated between 2004 and 2014 (Fig. 1). All patients were treated with PBT with passive scatter technology. Random sampling was performed by a biostatistitian (Y.I.). The patients were stratified into four categories according to whether they had cancers of (A) the brain, head and neck, (B) the chest, (C) the abdomen or (D) the whole central nervous system (WCNS). There were 157, 27, 42 and 16 patients in each category respectively. In each category, patients were again stratified according to sex (female or male), age (0–6 years old or 7–20 years old), and target volume (≤median, ≥median) to reduce the bias. After these stratifications, 8 patients were randomly selected from the patients in each of categories (A), (B) and (C). Since the number

Table 1. Schneider's fit parameters for the various dose–response models for carcinoma induction

Organ at risk	Linear model	Full model		Bell-shaped model	Plateau model	β_{JP}[b]	γ_e	γ_a
	β[b]	α[a]	R	α[a]	α[a]			
Brain	0.44	0.018	0.93	0.009	0.021	0.51	−0.024	2.38
Female breast		0.044	0.15	0.041	0.115	9.2	−0.037	1.7
Lung		0.042	0.83	0.022	0.056	7.5	0.002	4.23
Colon	7.2	0.001	0.99	0.001	0.001	8.0	−0.056	6.9
Stomach		0.46	0.46	0.111		9.5	−0.002	1.9
Small intestine		0.591	0.09	0.48		8.0	−0.056	6.9
Liver	0.22	0.323	0.29	0.243	0.798	4.3	−0.021	3.6
Bladder		0.219	0.06	0.213	0.633	3.2	−0.024	2.38
Thyroid				0.033		0.13	−0.046	0.6

[a]In Gy^{-1}.
[b]In $(10\,000\ PY\ Gy)^{-1}$. The parameters β, α and R are listed for each organ and each model. The β_{JP} is the initial slope of the A-bomb survivors for age at exposure of 30 and attained age of 70 years and age-modifying parameters γ_e and γ_α for various sites.

Table 2. Schneider's fit parameters for the various dose–response models for sarcoma induction

Organ at risk	Low repopulation			Intermediate repopulation			Full tissue recovery			γ_e	γ_a
	α[a]	R	β[b]	α[a]	R	β[b]	α[a]	R	β[b]		
Bone	0.019	0.1	1.7	0.067	0.5	0.2	0.078	1.0	0.1	−0.013	−0.56
Soft tissue	0.04	0.1	3.3	0.06	0.5	0.6	0.093	1.0	0.1	−0.013	−0.56

[a]In Gy^{-1}.
[b]In $(10\,000\ PY\ Gy)^{-1}$. The parameters β, α and R are listed for each organ and for three different values for R (0.1, 0.5 and 1.0). The γ_e and γ_a are the age-modifying parameters for various sites.

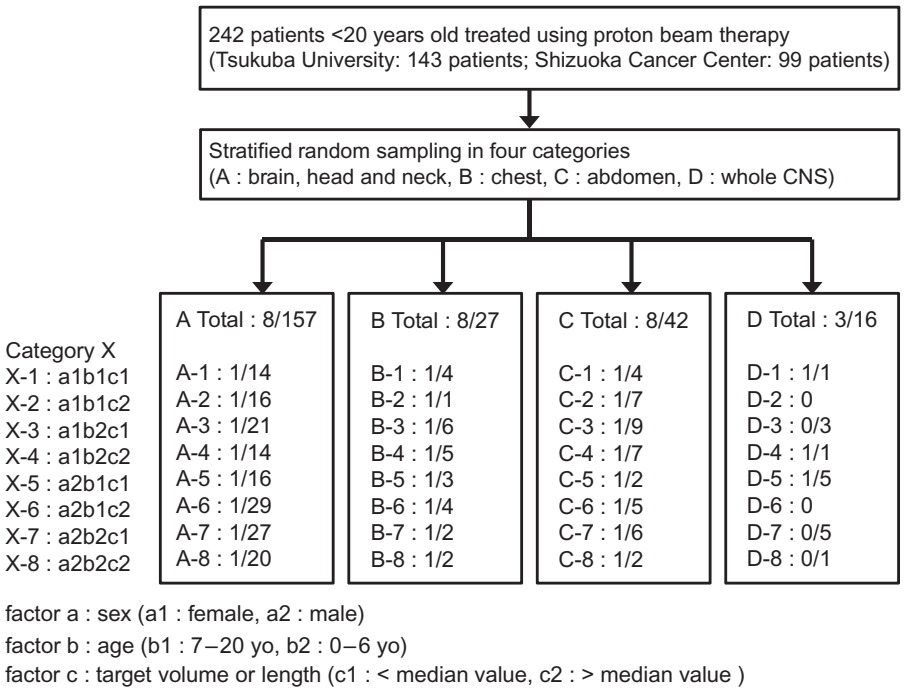

Figure 1. Schema of stratified random sampling from patients who had been treated using proton beam therapy at the Tsukuba University Hospital or Shizuoka Cancer Center.

of patients in category (D) who were treated by WCNS was too small to be randomly sampled, 1 female of age 11, 1 female of age 6, and 1 male of age 3 were selected to represent category (D). In total, 27 patients were selected by the biostatistician (Table 3).

An external committee consisting of three pediatric radiation oncologists who are experts in photon therapy assessed the appropriateness of the treatment planning of IMXT for the 27 patients. They evaluated simple clinical data, contouring of targets and OARs, dose–volume statistics (such as maximum and mean dose for each organ), dose–volume histograms, and dose distribution on CT image slice by slice. Two patients (sampling cases C-4, C-6) were required to be re-planned for IMXT to make the dose distribution better according to the assessment by the committee. Another patient in category A (sampling case A-5) was required to be deleted from subsequent analysis because the patient had been treated for a relapsed tumor after photon radiotherapy. Compatibility between IMXT and PBT was conducted in the 26 patients.

Statistical comparison

Digital data concerning the CT image, regions of interest (ROIs), 3D dose distribution, and DVH of the 26 patients were sent to the central office from each institution using the DICOM-RT format in principle. One of the authors (M.T.), who is a medical physicist, re-planned the IMXT for each patient using the dose constraint of each institution and the reference dose constraints from a previous paper [9]. It was assumed that 6-MV X-ray irradiation was to be used in IMXT. All the treatment planning for IMXT was based on the assessment by an external committee made up of three pediatric radiation oncologists, who used photon therapy to confirm that the re-planning of IMXT was not intentionally deteriorated and that its 3D dose distribution reached a standard level of conformity and uniformity. They confirmed that dose–volume statistics for the clinical target volume were equivalent between PBT and IMXT for all patients. After the approval of the external committee, the OED for each OAR, the EAR at the age attained, and the LAR for each patient were calculated for PBT and IMXT, respectively.

The mean and standard deviation among the patients in each category were calculated and compared using Student's *t*-test. The number needed to treat (NNT) was taken as the number of patients who required PBT instead of IMXT in order to prevent one additional incidence of radiation-induced secondary cancer. Since it is safe to assume that the LAR is smaller with PBT than IMXT for WCNS, where the irradiation volume is so different, a one tailed *t*-test is a reasonable assumption. For other regions, a two tailed *t*-test was used for comparison. P values < 0.05 were considered statistically significant. All statistical analyses were performed using JMP Pro® Version 12 (SAS Institute Inc., Cary, NC).

RESULTS

Calculation of the LARs of PBT and IMXT based on DVH was feasible for all patients.

The brain, thyroid, bone and soft tissue were selected as the OARs for PBT and IMXT for the seven patients with tumors of the brain, head and neck region. For bone and soft tissue, the parameters for sarcoma were used. If parameters for pleural models had been reported, parameters for each model were used to calculate

Table 3. Patient characteristics (category A: brain, head and neck; B: chest; C: abdomen; D: whole central nervous system), institutions, prescribed radiation dose, and fraction size

Patient	Primary pathology	Institution	Sex	Age (year)	Fractional dose (Gy)	No. of fractions	Prescribed dose (Gy)
A-1	Pontine glioma	Tsukuba	F	11	1.8	30	54
A-2	Germ cell tumor	Tsukuba	F	12	1.8	17	30.6
A-3	Ependymoma	Tsukuba	F	2	1.8	28	50.4
A-4	Ewing sarcoma	Tsukuba	F	2	1.8	28	50.4
A-6	Germ cell tumor	Tsukuba	M	16	1.8	28	50.4
A-7	Atypical teratoid/rhabdoid tumor	Tsukuba	M	2	1.8	32	57.6
A-8	Primitive neuroectodermal tumor	Shizuoka	M	2	1.8	28	50.4
B-1	Ewing sarcoma	Tsukuba	F	10	1.8	14	25.2
B-2	Pelvic bone, malignancy	Shizuoka	F	13	2.5	15	37.5
B-3	Rhabdomyosarcoma	Tsukuba	F	5	1.8	31	55.8
B-4	Neuroblastoma	Shizuoka	F	1	1.8	20	36
B-5	Pancreatoblastoma	Shizuoka	M	11	2.0	20	40
B-6	Ewing sarcoma	Tsukuba	M	19	2.5	24	60
B-7	Ependymoma	Tsukuba	M	3	1.8	28	50.4
B-8	Neuroblastoma	Shizuoka	M	3	1.8	20	36
C-1	Pancreatoblastoma	Tsukuba	F	11	2.5	24	60
C-2	Neuroblastoma	Shizuoka	F	8	1.8	20	36
C-3	Rhabdomyosarcoma	Tsukuba	F	2	1.8	25	45
C-4	Neuroblastoma	Tsukuba	F	3	1.8	17	30.6
C-5	Acinar cell carcinoma	Tsukuba	M	12	3.3	22	72.6
C-6	Ependymoma	Tsukuba	M	10	1.8	31	55.8
C-7	Neuroblastoma	Tsukuba	M	6	1.8	14	25.2
C-8	Neuroblastoma	Tsukuba	M	4	1.8	17	30.6
D-1	Medulloblastoma	Shizuoka	F	11	1.8	13	23.4
D-2	Medulloblastoma	Shizuoka	F	6	1.8	13	23.4
D-3	Medulloblastoma	Shizuoka	M	3	1.8	10	18

the LAR, and the load average value of LAR derived from both models was used. The difference in LAR between PBT and IMXT, or the LAR of IMXT minus that of PBT, was calculated for each OAR (Table 4). If we assume that the LAR of each organ is independent of the LAR of other organs, the cumulative risk of radiation-induced secondary cancer, or cumulative LAR, is calculated as the sum of the LAR of all organs in the same patient. We then assume that the LAR of other organs not in the planning CT scan was zero. The mean of the cumulative LAR of IMXT was significantly higher than that of PBT for the brain, bone and soft tissue (Table 4). The mean ± standard deviation was 1.02 ± 0.52%, and there was a statistical difference ($P = 0.0021$). The NNT was 98.0, suggesting that 1 out of 98 patients will not experience radiation-induced secondary cancer if we use PBT instead of IMXT.

The female breast, lung, colon, stomach, small intestine, liver, thyroid, bone and soft tissue were selected as the OARs for 8 patients with tumors of the thoracic region. The mean LAR of IMXT was significantly higher than that of PBT for the lung, stomach, liver, bone and soft tissue (Table 4). The mean ± standard

Table 4. LAR differences between PBT and IMXT and the number needed to treat (NNT) for each organ at risk (Category A: brain, head and neck; B: chest; C: abdomen; D: whole central nervous system)

Organ at risk	A. Brain, H&N			B. Chest			C. Abdomen			D. Whole CNS		
	LAR diff. (%)	NNT	*P* value	LAR diff. (%)	NNT	*P* value	LAR diff. (%)	NNT	*P* value	LAR diff. (%)	NNT	*P* value
Brain	0.77 ± 0.44	131	0.0036**							0.00 ± 0.01	-2.00×10^4	0.230
Female breast				7.46 ± 13.34	13.4	0.158	0.59 ± 1.19	171	0.207	15.9 ± 14.2	6.3	0.0960
Lung				3.23 ± 1.41	31.0	0.0003**				3.76 ± 2.59	26.6	0.0642
Colon				9.22 ± 14.96	10.8	0.125	12.5 ± 19.7	8.0	0.115	22.19 ± 6.94	4.5	0.0156*
Stomach				2.02 ± 1.95	49.6	0.0220*	1.89 ± 1.58	53.0	0.0118*	3.45 ± 2.44	29.0	0.0671
Small intestine				0.63 ± 0.78	160	0.0589	0.72 ± 0.80	139	0.0384*	2.30 ± 2.79	43.4	0.145
Liver				0.60 ± 0.42	166	0.0046**	0.49 ± 0.25	204	0.0009**	1.10 ± 0.14	90.6	0.0026**
Bladder							0.17 ± 0.32	584	0.171	0.14 ± 0.25	698	0.211
Thyroid	0.01 ± 0.01	1.89×10^4	0.356	−0.03 ± 0.13	-3.59×10^3	0.565				1.09 ± 0.18	91.8	0.0046**
Bone	0.08 ± 0.05	1.21×10^3	0.0043**	0.03 ± 0.04	2.95×10^3	0.0455*	0.08 ± 0.07	1.31×10^3	0.0183*	0.03 ± 0.02	3.23×10^3	0.0608
Soft tissue	0.17 ± 0.16	596	0.0335*	0.10 ± 0.09	1.03×10^3	0.0231*	0.20 ± 0.17	506	0.0121*			
Cumulative	1.02 ± 0.52	98.0	0.0021**	23.3 ± 17.2	4.3	0.0065**	16.6 ± 19.9	6.0	0.0497*	50.0 ± 21.1	2.0	0.0274*

A two-tailed *t*-test was used for Category A, B and C regions, and a one-tailed *t*-test was used for Category D. *P-value < 0.05 and >0.01, and **P-value <0.01.

deviation of the difference in cumulative LAR was 23.3 ± 17.2%, and the difference was statistically significant ($P = 0.0065$). The NNT was 4.3, suggesting that 1 out of 4.3 patients will not experience radiation-induced secondary cancer if we use PBT instead of IMXT.

The female breast, colon, stomach, small intestine, liver, bladder, bone and soft tissue were selected as the OARs for the 8 patients with cancers of the abdominal region. The mean LAR of IMXT was significantly higher than that of PBT for the stomach, small intestine, liver, bone and soft tissue. The mean ± standard deviation of the difference in cumulative LAR was 16.6 ± 19.9%, and there was a statistical difference ($P = 0.0497$). The NNT was 6.0.

For the 3 patients who were treated with WCNS, the brain, female breast, lung, colon, stomach, small intestine, liver, bladder, thyroid and bone were used as the OARs. The mean LAR of IMXT in the 3 patients was significantly higher than that of PBT for the colon, liver, and thyroid. The mean ± standard deviation of the cumulative LAR was 50.0 ± 21.1%, and the difference became statistically significant by one tailed *t*-test ($P = 0.0274$). The NNT was 2.0.

DISCUSSION

The relationship between exposure dose and radiation-induced secondary cancer has not been totally understood. However, the estimations derived from data on Japanese atomic bomb survivors are among the most reliable sources for understanding this relationship. Preston *et al.* analyzed the incidence of solid cancers among ~105 427 members of the Life Span Study (LSS) cohort of Hiroshima and Nagasaki atomic bomb survivors [5]. They found that 17 448 first primary cancers were diagnosed from 1958 through 1998. It was estimated that, at age 70 after an exposure at age 30, the solid cancer rates increased by ~35% per Gy [90% confidence interval (CI) 28%; 43%] for men and 58% per Gy (90% CI 43%; 69%) for women. For all solid cancers as a group, the excess relative risk (ERR per Gy) decreases by 17% per decade of increase in age at exposure (90% CI 7%; 25%) after allowing for attained-age effects, while the ERR decreased in proportion to the attained age to the power 1.65 (90% CI 2.1; 1.2) after allowing for age at exposure. The data were consistent with a linear dose response over the 0–2 Gy range, while there was some flattening of the dose response at higher doses. On the other hand, Dores *et al.* have examined secondary cancer incidence among long-term survivors of Hodgkin's disease, who were treated with a local dose of up to 40 Gy with mantle fields, by a population-based evaluation over 25 years [6]. Among 32 591 patients, there were 2153 secondary cancers reported, including 1726 solid tumors. The observed-to-expected ratio was 2.3 (95% CI 2.2; 2.4) for whole secondary cancers and 2.0 (95% CI 1.9; 2.0) for solid tumors. Schneider *et al.* have extensively examined the published data on A-bomb survivors in the low dose range, as well as the cancer risk data of Hodgkin's disease survivors in the high dose range. They also reconstructed the dose distribution of radiotherapy for Hodgkin's disease and estimated the most appropriate parameters to describe the relationship between the absorbed dose and the risk of secondary cancer in the dose range used in fractionated radiotherapy. Although there are still many uncertainties in the assumption of radiation-induced cancer in the radiotherapy dose range, their approach can be regarded as the most reasonable prediction model at present.

There is a possibility that the superiority of one technique relative to the others can not be predicted correctly by means of complex equations. For example, if the dose–response curve is not linear but bell-shaped, the higher dose around the target volume may not be associated with the increase in the risk of secondary cancer. In fact, the data are too sparse to select one dose–response model in many organs. Therefore, it is very important to use the LAR value with great caution. We think that (i) the LAR value will only be useful for comparing differences in the dose distribution in the same patient, (ii) all the dose–response models should be tested if there is no agreement in the selection of the dose–response models, (iii) faint differences in the LAR between different treatment techniques should not be regarded as solid differences, and (iv) statistical analysis should be carefully carried out with the help of biostatistics. In the future, if we can update the dose–response curve of the risk of secondary cancer, it may be possible to improve the use of the LAR derived from different dose–response models.

As long as we restrict ourselves to the policy above, the present study suggested that the LAR is useful for quantifying the difference in the risk of radiation-induced secondary cancer between two treatment techniques in the same patient. For 26 randomly selected pediatric patients who were treated with PBT, the risk of secondary cancer was suggested to be statistically lower than it would have been by treatment with IMXT. As far as we are aware, the number of patients in our study is the largest to date among studies that have estimated the risk of radiation-induced secondary cancer. The number of patients in the previous studies was 2, 2, 6, 10, 6 and 10 patients in Mirabell *et al.*, Paganetti *et al.*, Moteabbed *et al.*, Brodin *et al.*, Stokkevag *et al.* and Yoon *et al.* [1, 7–11], respectively. In this study, the difference was apparent for the thoracic and abdominal regions, but not for the brain and head and neck regions in general. These findings are consistent with the difference in the ratio of target volume to total irradiated volume to the patient between PBT and IMXT. Since the ratio of target volume to irradiated volume is large in patients who have received PBT for the brain and head and neck regions, the volume outside of the target volume was so small that no apparent difference was seen in the risk of secondary cancers. This relationship may not have been observed if PBT was used for the much smaller target volumes for the brain and head and neck regions. For the thoracic and abdominal regions, the volume outside the target volume was large enough to see the difference between PBT and IMXT. Again, this relationship may not have been observed if PBT was used for much larger target volume for the thoracic and abdominal regions. For WCNS irradiation, the difference was quite large.

One shortcoming of this study was that we did not include the effect of contaminated neutrons in PBT and in high-energy X-ray therapy. Both treatments are known to increase the contaminated neutrons compared with conventional conformal radiotherapy [22, 23]. The effect of neutron contamination should be investigated further because of the higher risk of secondary cancer of the neutrons. Newhauser *et al.* have reported that the effect of neutrons was small in spot-scanning PBT, although the effect was not negligible in

passive-scattering PBT [24]. Considering that spot-scanning PBT is becoming more common than passive-scattering PBT, neutrons are expected to have an increasingly diminished effect in PBT in clinical practice. It is also true that as volumetric multiple arc therapy (VMAT) becomes more popular in IMXT, the treatment time of IMXT and thus the contamination of neutrons will also be lowered in IMXT as well.

Another limitation of this study is that we did not completely validate the model used for the LAR calculation. We should follow up the patients very carefully for years after PBT and IMXT to confirm whether the differences predicted in this study are realized.

From the viewpoint of ALARA, the difference in the predicted risk of secondary cancer between the two treatments was so large that it is difficult to conduct a comparative study between PBT and IMXT for some areas. The difference was apparent for the patients who received WCNS, thoracic and abdominal irradiation. As long as the goal is to reduce the risk of secondary cancer after treatment for pediatric cancer, the present study suggested that PBT has been selected properly for these areas. For the treatment of the brain and head and neck regions, the difference in the risk of secondary cancer may not be as large as for the other regions. Difference in other late adverse reaction rates, such as vascular damage for pediatric patients between PBT and IMXT, should be investigated carefully. The total benefit of PBT should be determined by the total balance between the benefit and risk of various adverse reactions.

In conclusion, the LAR of radiation-induced secondary cancer was significantly lower when using PBT than when using IMXT for pediatric patients. The difference was apparent for the thoracic region, abdominal region and WCNS irradiation. The results suggested that it would be reasonable to use the cumulative LAR difference when we need to select between PBT and IMXT, not only for pediatric patients but also for other young adult patients. Even when other *in silico* surrogate markers, such as normal tissue complication probability and tumor control probability, do not differ between the two techniques, PBT would be the right choice for the treatment of pediatric patients in terms of LAR. However, more work is required for the precise estimation and long-term validation and updating of the models behind LAR estimation.

SUPPLEMENTARY DATA

Supplementary data are available at the *Journal of Radiation Research* online.

ACKNOWLEDGEMENTS

We appreciate the efforts of Dr Etsuyo Ogo, Dr Hiroshi Fuji and Dr Ei-ichi Masaki, who constituted the external committee for this study.

FUNDING

This research was supported by the Translational Research Network Program, the Japan Society for the Promotion of Science KAKENHI (Grant No. 15H04768) and the Global Institution for Collaborative Research and Education (GI-CoRE), Hokkaido University, founded by the Ministry of Education, Culture, Sports, Science and Technology (MEXT), Japan.

CONFLICT OF INTEREST

Dr Shirato received grants from Hitachi Co. Ltd, Mitsubishi Heavy Industry and Shimazu Co. Ltd, during the conduct of the study. In addition, Dr Shirato has a licensed US patent (6307914 B1). The remaining authors have declared no conflicts of interest.

REFERENCES

1. Miralbell R, Lomax A, Cella L, et al. Potential reduction of the incidence of radiation-induced second cancers by using proton beams in the treatment of pediatric tumors. *Int J Radiat Oncol Biol Phys* 2002;54:824–9.
2. Ng AK. Current survivorship recommendations for patients with Hodgkin lymphoma: focus on late effects. *Blood* 2014;124: 3373–9.
3. Langendijk JA, Lambin P, De Ruysscher D, et al. Selection of patients for radiotherapy with protons aiming at reduction of side effects: the model-based approach. *Radiother Oncol* 2013; 107:267–73.
4. Schneider U, Sumila M, Robotka J. Site-specific dose–response relationships for cancer induction from the combined Japanese A-bomb and Hodgkin cohorts for doses relevant to radiotherapy. *Theor Biol Med Model* 2011;8:27.
5. Preston DL, Ron E, Tokuoka S, et al. Solid cancer incidence in atomic bomb survivors: 1958–1998. *Radiat Res* 2007;168: 1–64.
6. Dores GM, Metayer C, Curtis RE, et al. Second malignant neoplasms among long-term survivors of Hodgkin's disease: a population-based evaluation over 25 years. *J Clin Oncol* 2002; 20: 3484–94.
7. Paganetti H, Athar BS, Moteabbed M, et al. Assessment of radiation-induced second cancer risks in proton therapy and IMRT for organs inside the primary radiation field. *Phys Med Biol* 2012;57: 6047–61.
8. Moteabbed M, Yock TI, Paganetti H. The risk of radiation-induced second cancers in the high to medium dose region: a comparison between passive and scanned proton therapy, IMRT and VMAT for pediatric patients with brain tumors. *Phys Med Biol* 2014;59:2883–99.
9. Brodin NP, Munck Af Rosenschöld P, Aznar MC, et al. Radiobiological risk estimates of adverse events and secondary cancer for proton and photon radiation therapy of pediatric medulloblastoma. *Acta Oncol* 2011;50:806–16.
10. Stokkevag CH, Engeseth GM, Ytre-Hauge KS, et al. Estimated risk of radiation-induced cancer following paediatric craniospinal irradiation with electron, photon and proton therapy. *Acta Oncol* 2014;53:1048–57.
11. Yoon M, Shin DH, Kim J, et al. Craniospinal irradiation techniques: a dosimetric comparison of proton beams with standard and advanced photon radiotherapy. *Int J Radiat Oncol Biol Phys* 2011;81:637–46.

12. Schneider U, Besserer J, Mack A. Hypofractionated radiotherapy has the potential for second cancer reduction. *Theor Biol Med Model* 2010;7:4.
13. Schneider U, Kaser-Hotz B. Radiation risk estimates after radiotherapy: application of the organ equivalent dose concept to plateau dose–response relationships. *Radiat Environ Biophys* 2005;44:235–9.
14. Schneider U, Kaser-Hotz B. A simple dose–response relationship for modeling secondary cancer incidence after radiotherapy. *Z Med Phys* 2005;15:31–7.
15. Schneider U, Zwahlen D, Ross D, et al. Estimation of radiation-induced cancer from three-dimensional dose distributions: concept of organ equivalent dose. *Int J Radiat Oncol Biol Phys* 2005;61:1510–5.
16. Hall EJ, Wuu CS. Radiation-induced second cancers: the impact of 3D-CRT and IMRT. *Int J Radiat Oncol Biol Phys* 2003;56:83–8.
17. Davis RH. Production and killing of second cancer precursor cells in radiation therapy: in regard to Hall and Wuu (*Int J Radiat Oncol Biol Phys* 2003;56:83–88). *Int J Radiat Oncol Biol Phys* 2004;59:916.
18. Schneider U. Mechanistic model of radiation-induced cancer after fractionated radiotherapy using the linear–quadratic formula. *Med Phys* 2009;36:1138.
19. Preston DL, Pierce DA, Shimizu Y, et al. Effect of recent changes in atomic bomb survivor dosimetry on cancer mortality risk estimates. *Radiat Res* 2004;162:377–89.
20. Schneider U, Walsh L. Cancer risk estimates from the combined Japanese A-bomb and Hodgkin cohorts for doses relevant to radiotherapy. *Radiat Environ Biophys* 2008;47:253–63.
21. The 2007 Recommendations of the International Commission on Radiological Protection. ICRP publication 103. *Annals of the ICRP* 2007;37(2–4):1–332.
22. Schneider U, Agosteo S, Pedroni E, et al. Secondary neutron dose during proton therapy using spot scanning. *Int J Radiat Oncol Biol Phys* 2002;53:244–51.
23. Yan X, Titt U, Koehler AM, et al. Measurement of neutron dose equivalent to proton therapy patients outside of the proton radiation field. *Nucl Instrum Methods Phys Res A* 2002;476:429–34.
24. Newhauser WD, Fontenot JD, Mahajan A, et al. The risk of developing a second cancer after receiving craniospinal proton irradiation. *Phys Med Biol* 2009;54:2277–91.

APPENDIX A. RISK EQUIVALENT DOSE (RED)

A.1 DOSE–RESPONSE MODELS FOR CARCINOMA INDUCTION

Dose–response models for carcinoma induction by radiation are expressed by three models: A.1.1, A.1.2 and A.1.3 in principle. A.1.4 is the model proposed by Schneider *et al.* The risk equivalent dose (RED) is defined as the dose that produces the equivalent risk of inducing cancer. RED is the dose that changes with OARs and the daily dose in fractionated irradiation.

A.1.1 LINEAR MODEL

$$RED(D) = D \tag{A1}$$

A.1.2 BELL-SHAPED MODEL ($R \to 0$)

$$RED(D) = D\ e^{-\alpha' D} \tag{A2}$$

A.1.3 PLATEAU MODEL ($R \to 1$)

$$RED(D) = \frac{e^{-\alpha' D}}{\alpha'} \tag{A3}$$

A.1.4 FULL MODEL

$$RED(D) = \frac{e^{-\alpha' D}}{\alpha' R}\left(-1 - 2R + R^2 e^{\alpha' D} - 1(1-R)^2 e^{-\frac{\alpha' R}{1-R} D}\right) \tag{A4}$$

$$\alpha' = \alpha + \beta \frac{d_f}{D_T} D$$

D: dose; R, α': organ-specific model parameters
(R: repopulation parameter; α' : cell kill parameter);
D_T: prescribed dose; d_f: fraction dose.

A.2 DOSE–RESPONSE MODELS FOR SARCOMA INDUCTION

For sarcoma induction, the following formula was used:

$$RED(D) = \frac{e^{-\alpha' D}}{\alpha' R}\left(-1 - 2R + R^2 e^{\alpha' D} - 1(1-R)^2 e^{-\frac{\alpha' R}{1-R}} - \alpha' RD\right). \tag{A5}$$

A dose–response model in case of full repopulation/repair is derived by taking Eq. A4 to the limit of $R = 1$:

$$RED(D) = \frac{e^{-\alpha' D}}{\alpha' R}(-1 - \alpha' D + e^{\alpha' D}). \tag{A6}$$